Semi-automatic Segmentation of Vertebral Bodies in Volumetric MR Images Using a Statistical Shape+Pose Model

Amin Suzani[a], Abtin Rasoulian[a], Sidney Fels[a], Robert N. Rohling[a,b], and Purang Abolmaesumi[a]

[a] Department of Electrical and Computer Engineering, University of British Columbia, Vancouver, BC, CANADA

[b] Department of Mechanical Engineering, University of British Columbia, Vancouver, BC, CANADA

ABSTRACT

Segmentation of vertebral structures in magnetic resonance (MR) images is challenging because of poor contrast between bone surfaces and surrounding soft tissue. This paper describes a semi-automatic method for segmenting vertebral bodies in multi-slice MR images. In order to achieve a fast and reliable segmentation, the method takes advantage of the correlation between shape and pose of different vertebrae in the same patient by using a statistical multi-vertebrae anatomical shape+pose model. Given a set of MR images of the spine, we initially reduce the intensity inhomogeneity in the images by using an intensity-correction algorithm. Then a 3D anisotropic diffusion filter smooths the images. Afterwards, we extract edges from a relatively small region of the pre-processed image with a simple user interaction. Subsequently, an iterative Expectation Maximization technique is used to register the statistical multi-vertebrae anatomical model to the extracted edge points in order to achieve a fast and reliable segmentation for lumbar vertebral bodies. We evaluate our method in terms of speed and accuracy by applying it to volumetric MR images of the spine acquired from nine patients. Quantitative and visual results demonstrate that the method is promising for segmentation of vertebral bodies in volumetric MR images.

Keywords: Segmentation, vertebral body, volumetric MR image, multi-vertebrae anatomical model.

1. INTRODUCTION

Segmentation of vertebral structures in volumetric medical images of the spine is an essential step in the design of computer aided diagnosis systems for measuring the deformations caused by different spinal pathologies such as osteoporosis, spinal stenosis, spondylolisthesis and scoliosis. When making decisions for diagnosis and therapy of these pathologies, physicians often use magnetic resonance (MR) images for the assessment of soft spinal structures such as inter-vertebral discs and nerve roots. However, the established methods for segmentation of vertebral structures have been mainly developed for computed tomography (CT). CT, on the other hand, requires radiation exposure and does not depict soft tissue as well as MR images. The availability of a fast and reliable spine segmentation of MR images may eliminate the need for CT and benefit patient care.

Segmentation of vertebral structures in MR images is challenging, mainly due to poor contrast between bone surfaces and surrounding soft tissue. Another challenge is relatively large inter-slice gap (more than 3 mm) in typical clinical MR images compared to CT. In addition, spatial variations in surrounding soft tissue contrast and magnetic field inhomogeneities increase the complexity of the segmentation task in MR images.

For spine segmentation in MR images, several methods have been proposed in the literature. Most of them are 2D approaches that are applied on manually identified cross-sections which contain the target vertebrae[1–4]. Peng et al.[5] search for the best slice automatically and then perform a 2D segmentation approach. A smaller number of methods have been proposed for MR segmentation of vertebral structures in 3D. The method from Hoad et al.[6] has a labour-intensive initialization step and also a post-processing step for correcting the segmentation. Štern et al.[7,8] perform the segmentation by optimizing the parameters of a geometrical model of vertebral bodies. The method from Neubert et al.[9] uses statistical shape models and registration of grey level intensity profiles

for vertebral body segmentation. Methods from Hoad et al. and Štern et al. have long execution times (at least more than five minutes for high-resolution volumetric images). All three above-stated 3D approaches segment each vertebra independently. Consequently, the correlation between shapes of different vertebrae in a patient is disregarded. In addition, all above-mentioned methods for 3D segmentation are evaluated on volumetric images with an inter-slice gap of at most 1.2 mm which is not commonly used in clinical practice. Recently, a method was proposed by Kadoury et al.[10] for spine segmentation using Manifold embeddings. Multiple vertebrae are treated as a whole shape in this work. However, it is still evaluated on MR images with less than 1.2 mm slice thickness, and no computation time was reported.

In our previous work, we have successfully segmented lumbar vertebrae in volumetric CT scans using a statistical multi-vertebrae anatomical shape+pose model[11,12]. In this work, we aim to find simple and fast pre-processing steps to overcome the MR segmentation challenges explained above, and consequently obtain edge points of vertebral bodies from widely spaced slices of routine volumetric MR images. Thereafter, we register our multi-vertebrae anatomical model to the extracted edge points with the goal of achieving a fast and reliable segmentation of lumbar vertebral bodies in MR images.

2. MATERIALS

The performance of the proposed method was evaluated on T1-weighted MR images of nine patients (via SpineWeb[13]). The in-plane resolution is 0.5×0.5 mm^2 with a slice spacing between 3.3 to 4.4 mm. Each series of images consists of slices with 512×512 pixels. The number of slices from each patient ranges from 12 to 18. The multi-vertebrae anatomical model was constructed from manually segmented volumetric CT scans of an independent group of 32 subjects[11,12]. Ground truth segmentations were obtained manually using ITK-SNAP[14].

3. METHODS

3.1 Intensity Correction

The presence of intensity inhomogeneity in spinal MR images can adversely influence the ability to extract edges. Hence, we first apply an intensity correction algorithm on MR images to reduce this inhomogeneity. The bias field correction function provided in Statistical Parametric Mapping software package (SPM12b, Wellcome Department of Cognitive Neurology, London, UK) is used for this purpose. Figures 1(a) and 1(b), respectively, show the mid-sagittal slice of a sample MR image before and after intensity correction.

3.2 Anisotropic diffusion

We then apply a conventional 3D anisotropic diffusion[15] filter to the intensity-corrected image. Anisotropic diffusion is an image smoothing algorithm that attempts to preserve edges. Figures 1(b) and 1(c), respectively, show the image before and after this step. The function below (proposed by Perona and Malik[15]) is used for the diffusion coefficient in order to privilege high-contrast edges over low-contrast ones.

$$c(x, y, z, t) = e^{-(||\nabla I||/\kappa)^2}, \tag{1}$$

∇I denotes the image gradient, and the conductance parameter, κ, controls the sensitivity to edges. Weak edges can block the conductance when κ is too low, and strong edges may not be preserved when κ is too high. In all experiments κ and the integration constant, Δt, were set to 50 and 1/7, respectively. The algorithm was run with 20 iterations for each volumetric image.

3.3 Canny edge detection

At this step, the intensity-corrected mid-sagittal slice of the image is shown to the user. The user clicks on each of the lumbar vertebrae (L1 to L5) in the image (five points in total). For some irregular image acquisitions where those vertebrae are not visible in the mid-sagittal slice, the user could select a slice manually to be able to click on the vertebrae. However, we do not observe any sensitivity to the slice selection. Only the clicked points are used for the rest of the procedure. After user interaction, the Canny edge detection algorithm is applied to find the edge map of vertebral bodies in potential regions of the volumetric image. These regions are five cubic

bounding boxes centered at the clicked points. The scales of the cubes are obtained from the average distance of consecutive user clicks. The sensitivity threshold of the Canny edge detector is obtained automatically based on the maximum value of the gradient magnitude of the region. Figure 2 shows the result of edge detection in mid-sagittal slice of three different volumetric MR images. The statistical model is registered to the edge map obtained from this step.

3.4 Segmentation Using the Multi-vertebrae Model

Variations of shapes and poses of lumbar vertebrae were independently extracted from previously acquired 32 manually-segmented volumetric CT images[11]. This analysis was performed on all five lumbar vertebrae combined, taking into account the correlation between shapes of different vertebrae. The extracted variations are then represented in a statistical model. An iterative Expectation Maximization (EM) registration technique presented by Rasoulian et al.[11] is used for aligning the model to the edge points extracted from MR images in the previous step.

4. RESULTS AND DISCUSSION

Our segmentation results are quantitatively evaluated by using the manual segmentation as the ground truth. The mean error and Hausdorff distance are reported for each vertebra in a volumetric image (Table 1). For each point of the 3D surface mesh of manual segmentation we find its distance to the closest point in the registered model. The average of these distances is considered as the mean error and the maximum of them is considered as the Hausdorff distance. In order to make our results comparable with other approaches that only focus on 2D segmentation[1–4], we also report the segmentation errors for the 2D mid-sagittal slice of each image in Table 2. Some examples of our segmentation results are shown in Figure 3. Although the slice spacing in our MR images is relatively high (between 3.3 and 4.4 mm), the quantitative results show that our method can segment the lumbar vertebral bodies in MR images with a mean error of $\sim$3 mm. The overall segmentation for each image takes less than 2 minutes using our implementation in MATLAB (The MathWorks, Inc., Natick, MA) on a 2.5 GHz Intel core i5 machine.

Table 1. Mean error and maximum distance (Hausdorff) of 3D segmentation in each multi-slice image are reported (in mm) for each vertebral body.

Subject	L1		L2		L3		L4		L5		All lumbar vertebrae	
	Mean	Max	Mean	Max	Mean	Max	Mean	Max	Mean	Max	Mean ± std	Max
1	2.6	6.5	2.2	6.7	2.1	5.9	2.2	7.7	2.6	8.3	2.3 ± 0.2	8.3
2	2.9	9.8	2.8	8.1	2.4	7.3	3.1	11.3	2.9	9.1	2.8 ± 0.3	11.3
3	2.8	7.1	2.1	5.7	2.0	6.5	2.8	6.0	3.0	8.5	2.5 ± 0.4	8.5
4	2.7	7.5	3.7	9.6	3.8	9.6	4.0	10.3	3.7	12.4	3.6 ± 0.5	12.4
5	2.6	7.4	2.4	8.5	2.5	8.8	2.6	9.3	3.3	11.1	2.7 ± 0.4	11.1
6	1.9	6.4	2.3	7.0	2.9	10.2	3.2	12.3	3.0	12.1	2.7 ± 0.5	12.3
7	3.6	11.6	4.1	12.0	3.7	11.1	4.4	11.4	5.1	13.2	4.2 ± 0.6	13.2
8	2.5	6.7	3.3	11.7	5.9	16.3	4.0	12.8	2.6	7.2	3.7 ± 1.4	16.3
9	2.0	6.3	2.3	6.6	3.0	9.5	3.3	11.7	2.7	8.9	2.7 ± 0.5	11.7
Average	2.6	7.7	2.8	8.4	3.1	9.4	3.3	10.3	3.2	10.1	3.0 ± 0.8	11.7

5. CONCLUSION

A semi-automatic segmentation algorithm based on registering a statistical model is applied on nine 3D MR images of spine. Adding simple MR pre-processing steps allows the multi-vertebrae shape+pose model developed previously for CT scans to work on volumetric MR images. The statistical model can accommodate large inter-slice gaps. In addition, it is fast because it exploits the fact that neighbouring vertebrae have similar shapes and poses. The segmentation error will determine the range of clinical applications of this method, but will include display protocols in radiology workstations, automatic curved reformatting and 3D spinal visualization.

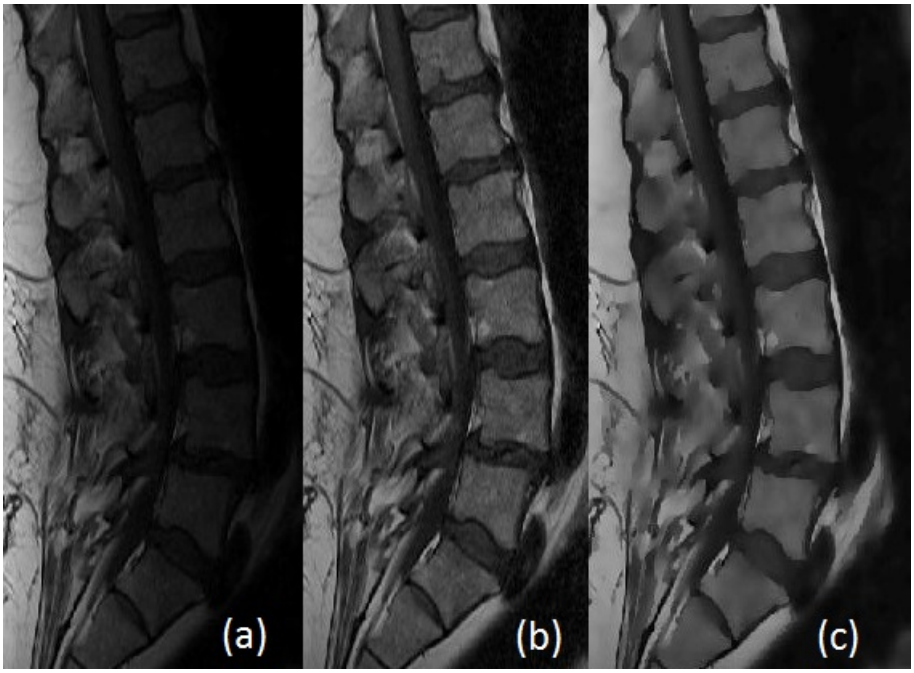

Figure 1. (a) Mid-sagittal slice of original image, (b) after intensity-correction, (c) after intensity correction and anisotropic diffusion.

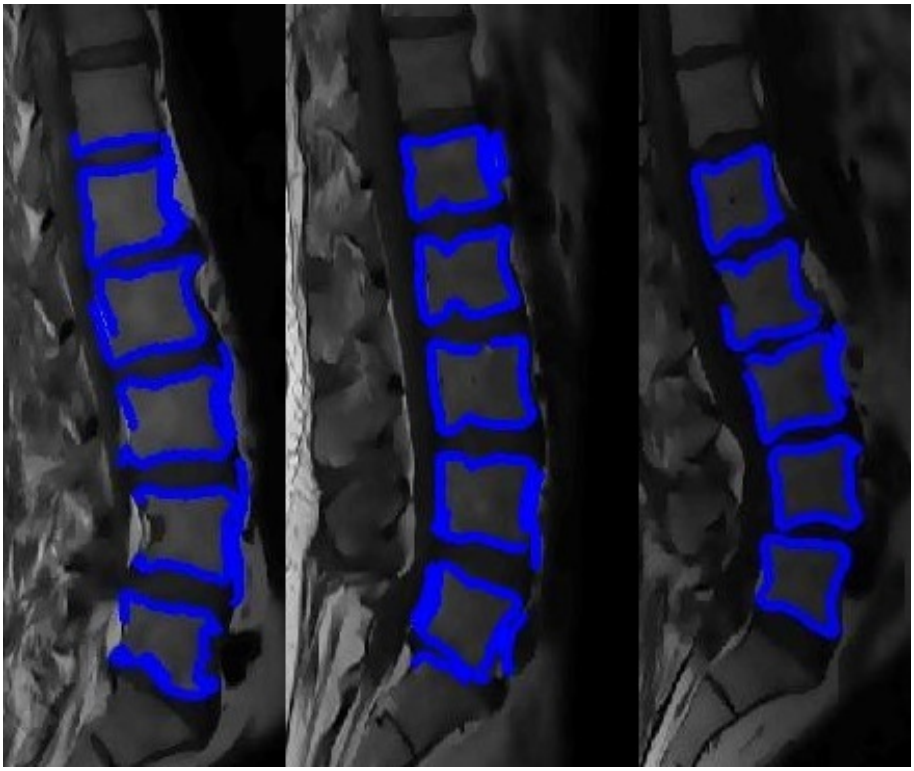

Figure 2. Edge extraction results in mid-sagittal slice of three different volumes.

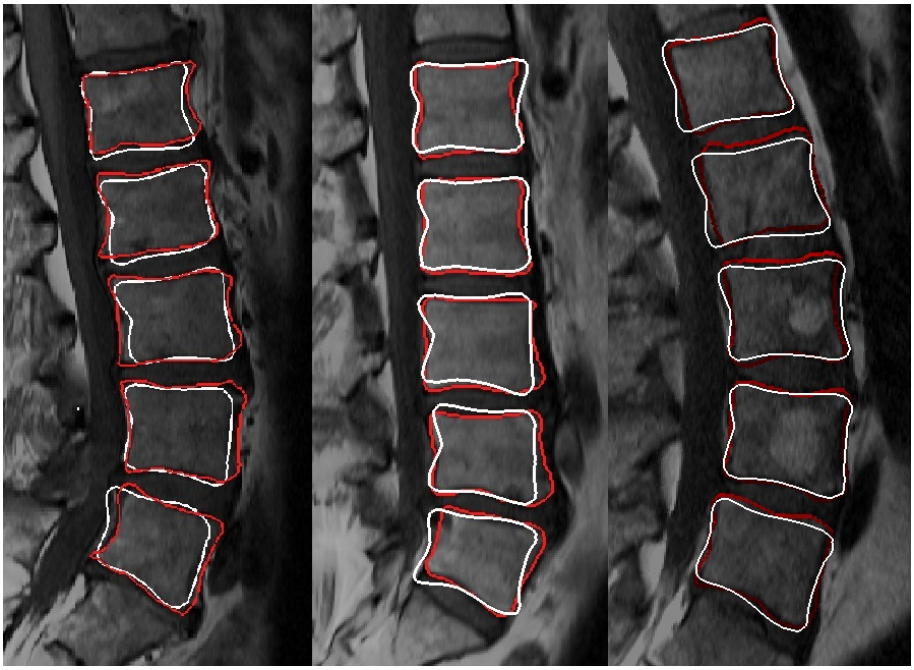

Figure 3. Examples of segmentation results in three different subjects. White contours show our segmentation results, while manual segmentation is shown with red contours.

Table 2. Mean error and maximum distance (Hausdorff) of 2D segmentation in the mid-sagittal slice of each image are reported (in mm) for each vertebral body.

Subject	L1		L2		L3		L4		L5		All lumbar vertebrae	
	Mean	Max	Mean	Max	Mean	Max	Mean	Max	Mean	Max	Mean ± std	Max
1	1.6	3.7	1.6	4.2	1.4	2.9	1.6	2.8	1.3	2.5	1.5 ± 0.1	4.2
2	1.6	3.6	2.1	4.3	1.7	3.5	2.3	4.2	2.0	4.1	2.0 ± 0.3	4.3
3	1.4	2.5	1.4	2.4	1.6	2.6	2.1	4.4	3.0	5.8	1.9 ± 0.7	5.8
4	1.7	4.4	1.8	4.3	1.7	4.6	2.1	4.8	2.3	5.3	1.9 ± 0.3	5.3
5	2.2	5.4	2.4	5.3	2.3	7.2	2.7	9.5	2.8	7.1	2.5 ± 0.3	9.5
6	1.6	4.0	1.5	2.6	1.5	3.6	1.8	5.0	1.7	3.6	1.6 ± 0.1	5.0
7	2.1	4.1	1.7	4.6	1.6	3.6	1.9	4.7	2.5	7.1	2.0 ± 0.3	7.1
8	1.9	4.9	2.3	5.7	1.9	5.2	2.8	7.4	2.2	5.1	2.2 ± 0.4	7.4
9	1.9	4.5	1.5	2.7	1.5	3.1	2.5	5.5	1.5	2.7	1.8 ± 0.4	5.5
Average	1.8	4.1	1.8	4.0	1.7	4.0	2.2	5.4	2.2	4.8	1.9 ± 0.4	6.0

Future work will concentrate on using the registered model for segmentation of whole vertebrae, and also make the process fully automatic. The evaluation will be improved by using segmented CT scans of same patients as the ground truth for MR segmentation since the manual segmentation of MR images is a subjective task.

6. ACKNOWLEDGEMENT

This work is funded in part by the Natural Sciences and Engineering Research Council of Canada (NSERC), and the Canadian Institutes of Health Research (CIHR). The MR data is generously provided by Dr. Shuo Li, GE Health Research, Ontario, Canada.

REFERENCES

[1] Egger, J., Kapur, T., Dukatz, T., Kolodziej, M., Zukić, D., Freisleben, B., and Nimsky, C., "Square-cut: a segmentation algorithm on the basis of a rectangle shape," *PloS One* **7**(2), e31064 (2012).

[2] Carballido-Gamio, J., Belongie, S. J., and Majumdar, S., "Normalized cuts in 3-D for spinal MRI segmentation," *Medical Imaging, IEEE Transactions on* **23**(1), 36–44 (2004).

[3] Shi, R., Sun, D., Qiu, Z., and Weiss, K. L., "An efficient method for segmentation of MRI spine images," in [*Complex Medical Engineering, 2007. CME 2007. IEEE/ICME International Conference on*], 713–717, IEEE (2007).

[4] Huang, S.-H., Chu, Y.-H., Lai, S.-H., and Novak, C. L., "Learning-based vertebra detection and iterative normalized-cut segmentation for spinal MRI," *Medical Imaging, IEEE Transactions on* **28**(10), 1595–1605 (2009).

[5] Peng, Z., Zhong, J., Wee, W., and Lee, J.-h., "Automated vertebra detection and segmentation from the whole spine MR images," in [*Engineering in Medicine and Biology Society, 2005. IEEE-EMBS 2005. 27th Annual International Conference of the*], 2527–2530, IEEE (2006).

[6] Hoad, C. and Martel, A., "Segmentation of MR images for computer-assisted surgery of the lumbar spine," *Physics in Medicine and Biology* **47**(19), 3503 (2002).

[7] Štern, D., Vrtovec, T., Pernuš, F., and Likar, B., "Segmentation of vertebral bodies in CT and MR images based on 3D deterministic models," in [*SPIE Medical Imaging*], 79620D–79620D, International Society for Optics and Photonics (2011).

[8] Štern, D., Likar, B., Pernuš, F., and Vrtovec, T., "Parametric modelling and segmentation of vertebral bodies in 3D CT and MR spine images," *Physics in Medicine and Biology* **56**(23), 7505 (2011).

[9] Neubert, A., Fripp, J., Engstrom, C., Schwarz, R., Lauer, L., Salvado, O., and Crozier, S., "Automated detection, 3D segmentation and analysis of high resolution spine MR images using statistical shape models," *Physics in Medicine and Biology* **57**(24), 8357 (2012).

[10] Kadoury, S., Labelle, H., and Paragios, N., "Spine segmentation in medical images using manifold embeddings and higher-order MRFs," *Medical Imaging, IEEE Transactions on* **32**(7), 1227–1238 (2013).

[11] Rasoulian, A., Rohling, R., and Abolmaesumi, P., "Lumbar spine segmentation using a statistical multi-vertebrae anatomical shape+ pose model," *Medical Imaging, IEEE Transactions on* (in press).

[12] Rasoulian, A., Rohling, R. N., and Abolmaesumi, P., "A statistical multi-vertebrae shape+ pose model for segmentation of CT images," in [*SPIE Medical Imaging*], 86710P–86710P, International Society for Optics and Photonics (2013).

[13] Yao, J., Burns, J. E., Munoz, H., and Summers, R. M., "Detection of vertebral body fractures based on cortical shell unwrapping," in [*Medical Image Computing and Computer-Assisted Intervention–MICCAI 2012*], 509–516, Springer (2012).

[14] Yushkevich, P. A., Piven, J., Cody Hazlett, H., Gimpel Smith, R., Ho, S., Gee, J. C., and Gerig, G., "User-guided 3D active contour segmentation of anatomical structures: Significantly improved efficiency and reliability," *Neuroimage* **31**(3), 1116–1128 (2006).

[15] Perona, P. and Malik, J., "Scale-space and edge detection using anisotropic diffusion," *Pattern Analysis and Machine Intelligence, IEEE Transactions on* **12**(7), 629–639 (1990).